Development 138, 4199-4205 (2011) doi:10.1242/dev.064261

The novel transmembrane protein Tmem2 is essential for coordination of myocardial and endocardial morphogenesis

Ronald Totong[1], Thomas Schell[1], Fabienne Lescroart[1], Lucile Ryckebüsch[2], Yi-Fan Lin[1,2], Tomasz Zygmunt[1], Lukas Herwig[3], Alice Krudewig[3], Dafna Gershoony[4], Heinz-Georg Belting[3], Markus Affolter[3], Jesús Torres-Vázquez[1] and Deborah Yelon[1,2,*]

SUMMARY

Coordination between adjacent tissues plays a crucial role during the morphogenesis of developing organs. In the embryonic heart, two tissues – the myocardium and the endocardium – are closely juxtaposed throughout their development. Myocardial and endocardial cells originate in neighboring regions of the lateral mesoderm, migrate medially in a synchronized fashion, collaborate to create concentric layers of the heart tube, and communicate during formation of the atrioventricular canal. Here, we identify a novel transmembrane protein, Tmem2, that has important functions during both myocardial and endocardial morphogenesis. We find that the zebrafish mutation *frozen ventricle* (*frv*) causes ectopic atrioventricular canal characteristics in the ventricular myocardium and endocardium, indicating a role of *frv* in the regional restriction of atrioventricular canal differentiation. Furthermore, in maternal-zygotic *frv* mutants, both myocardial and endocardial cells fail to move to the midline normally, indicating that *frv* facilitates cardiac fusion. Positional cloning reveals that the *frv* locus encodes Tmem2, a predicted type II single-pass transmembrane protein. Homologs of Tmem2 are present in all examined vertebrate genomes, but nothing is known about its molecular or cellular function in any context. By employing transgenes to drive tissue-specific expression of *tmem2*, we find that Tmem2 can function in the endocardium to repress atrioventricular differentiation within the ventricle. Additionally, Tmem2 can function in the myocardium to promote the medial movement of both myocardial and endocardial cells. Together, our data reveal that Tmem2 is an essential mediator of myocardium-endocardium coordination during cardiac morphogenesis.

KEY WORDS: Zebrafish, Heart development, Atrioventricular canal, Cardiac fusion

INTRODUCTION

The embryonic heart tube is initially a two-layered structure: the outer layer of muscular myocardium contracts to propel circulation and the inner layer of endothelial endocardium provides continuity with the rest of the vasculature. Myocardial and endocardial cells originate in neighboring regions of the lateral mesoderm (Schoenebeck et al., 2007). During the process of cardiac fusion, both cell types migrate medially in a synchronized fashion and merge at the midline to assemble the heart tube (Bussmann et al., 2007; Holtzman et al., 2007; Moreno-Rodriguez et al., 2006). At later stages, cardiac maturation involves remodeling of both juxtaposed layers during valve formation and trabeculation (Armstrong and Bischoff, 2004; Hinton and Yutzey, 2010; Sedmera et al., 2000). Despite the continual proximity of the myocardium and endocardium, little is known about the mechanisms that coordinate their development.

The coordination of myocardial and endocardial development has been particularly well established in the context of atrioventricular canal (AVC) formation. Both the myocardium and endocardium undergo specialized differentiation in order to create the characteristic morphology of the AVC and to establish the endocardial cushions that will remodel into the atrioventricular valve (Armstrong and Bischoff, 2004; Beis et al., 2005; Chi et al., 2008; Hinton and Yutzey, 2010). Several studies indicate that myocardium-endocardium communication regulates these spatially coincident events (Armstrong and Bischoff, 2004; Hinton and Yutzey, 2010). For example, chick explant experiments suggest that signal transduction between atrioventricular myocardium and atrioventricular endocardium induces endocardial cushion formation (Mjaatvedt et al., 1987). Although several signaling pathways have been implicated in promoting endocardial cushion development (Armstrong and Bischoff, 2004; Beis et al., 2005; Hinton and Yutzey, 2010), it is less clear which genes are responsible for attenuating these signals so as to spatially restrict atrioventricular differentiation.

Myocardium-endocardium coordination is also crucial during cardiac fusion. The synchronization of myocardial and endocardial migration suggests that both tissues respond to the same cues in the extracellular environment. Some cues may emanate from the endoderm: both myocardial and endocardial fusion are inhibited when endodermal specification or morphogenesis is disrupted (e.g. Holtzman et al., 2007; Kikuchi et al., 2001; Kupperman et al., 2000). Additionally, either diminished or excessive deposition of extracellular matrix (ECM) can hinder myocardial and endocardial movement (e.g. Arrington and Yost, 2009; Garavito-Aguilar et al., 2010; Trinh and Stainier, 2004). Furthermore, the myocardium and endocardium may impact the behavior of one another. Cardiomyocytes display aberrant migration patterns in the absence

[1]Developmental Genetics Program and Department of Cell Biology, Kimmel Center for Biology and Medicine, Skirball Institute of Biomolecular Medicine, New York University School of Medicine, New York, NY 10016, USA. [2]Division of Biological Sciences, University of California, San Diego, La Jolla, CA 92093, USA. [3]Biozentrum, University of Basel, CH-4056 Basel, Switzerland. [4]Department of Pharmacology, New York University School of Medicine, New York, NY 10016, USA.

*Author for correspondence (dyelon@ucsd.edu)

Accepted 18 July 2011

of endocardial cells, implying that myocardium-endocardium communication influences the direction of cell movement (Holtzman et al., 2007). However, the molecular basis for myocardium-endocardium interactions during cardiac fusion is not yet clear.

To elucidate the molecular mechanisms underlying myocardium-endocardium communication, we have investigated the zebrafish mutation *frozen ventricle* (*frv*). Zygotic *frv* mutants display ectopic AVC characteristics, and maternal-zygotic *frv* mutants exhibit defects in cardiac fusion. Positional cloning indicates that the *frv* locus encodes Tmem2, a previously uncharacterized transmembrane protein. Tissue-specific rescue experiments suggest that Tmem2 acts in the endocardium to spatially restrict atrioventricular differentiation, whereas during cardiac fusion Tmem2 acts in the myocardium to promote the medial movement of both myocardial and endocardial cells. Together, our studies illuminate crucial roles of a novel molecule, Tmem2, in regulating the coordination of myocardial and endocardial morphogenesis.

MATERIALS AND METHODS

Zebrafish

We discovered the recessive lethal mutation *frozen ventricle* (*frv*^{sk38}) through routine intercrosses in the Skirball zebrafish facility. To obtain maternal-zygotic *frv* embryos, we generated germline replacement chimeras through transplantation, as previously described (Ciruna et al., 2002). Donor embryos were generated by intercrossing *frv* heterozygotes, and wild-type host embryos were screened for germ cells derived from *frv*$^{-/-}$ donors. We raised 273 chimeric embryos and recovered eight fertile adult females. These females were bred to male *frv* heterozygotes to generate maternal-zygotic *frv* mutants.

In situ hybridization

We conducted in situ hybridization using previously reported probes for *myl7* (ZDB-GENE-991019-3), *notch1b* (ZDB-GENE-990415-183), *bmp4* (ZDB-GENE-980528-2059), *versican* (ZDB-GENE-011023-1), *tbx2b* (ZDB-GENE-990726-27) and *cdh5* (ZDB-GENE-040816-1). Mutant embryos were identified by PCR genotyping.

Immunofluorescence

We performed MF20/S46 whole-mount immunofluorescence as previously described (Alexander et al., 1998). To detect Dm-grasp, we used the monoclonal antibody zn-5 (ZIRC; 1:10), rabbit polyclonal anti-GFP (Invitrogen; 1:100), goat anti-mouse IgG Alexa 594 (Invitrogen; 1:100) and goat anti-rabbit IgG Alexa 488 (Invitrogen; 1:100). Embryos were fixed in 4% PFA at 4°C overnight and were cut coronally posterior to the common cardinal vein to facilitate antibody penetration. Staining was performed in PBS with 0.5% Triton X-100 and 1% DMSO. Confocal images were obtained using a Zeiss LSM510 microscope, and *z*-stacks were rendered in three dimensions and analyzed with Volocity software (Perkin Elmer).

Positional cloning of *frv*

Meiotic mapping demonstrated that the *frv* mutation is located on chromosome 5, between SSLP markers z61852 and z22523. Analysis of SNPs narrowed the interval to a region containing five candidate genes. Sequencing of the coding region of *tmem2* (GenBank HQ997922) revealed a nonsense mutation in *frv*.

mRNA and morpholino injection

Embryos were injected at the one-cell stage with 200-500 pg mRNA or 8-13.5 ng anti-*tmem2* morpholino (MO) (5′-AGCAGTCCAAGCATACC-ATTACTCC-3′; Gene Tools). Capped mRNA was synthesized from a pCS2 vector containing the *tmem2* or *tmem2-gfp* coding sequence. The MO blocks splicing between exon 4 and intron 4-5, which is predicted to result in a truncated protein that contains the first 404 amino acids of Tmem2 and 44 amino acids encoded by intronic sequence.

Transgenes

We used the Gateway system (Kwan et al., 2007; Villefranc et al., 2007) to create the transgenes *Tg(myl7:tmem2-gfp)*, *Tg(kdrl:gal4vp16)* and *Tg(uas:tmem2-gfp)*. We employed Tol2 transposase-mediated transgenesis for both transient transgene expression and generation of transgenic founders (Fisher et al., 2006). Additional transgenic lines used were *Tg(kdrl:GRCFP)* (Cross et al., 2003) and *Tg(fliep:gal4ff)*^{ubs4}, which drives endothelium-specific expression of the GAL4-VP16 derivative Gal4FF and is described elsewhere (Zygmunt et al., 2011).

RESULTS AND DISCUSSION

frv restricts atrioventricular differentiation to the atrioventricular canal

The zebrafish mutation *frozen ventricle* (*frv*) has a distinctive impact on cardiac morphology and function. At 48 hours post-fertilization (hpf), embryos homozygous for *frv* exhibited contractility and dysmorphic cardiac chambers, with poor demarcation of the AVC and an abnormal separation between the ventricular myocardium and endocardium (Fig. 1A-H). By 72 hpf, the *frv* mutant ventricle ceased to contract, although atrial function seemed unaffected, inspiring the use of *frozen ventricle* as the locus name.

Expression patterns of cardiac genes appeared normal during the initial steps of heart tube assembly in *frv* mutants (see Fig. S1 in the supplementary material). By contrast, defects in expression of the AVC markers *notch1b*, *bmp4*, *versican*, and *tbx2b* were evident in *frv* mutants by 48 hpf. In wild-type embryos, expression of each of these markers becomes restricted to the AVC (Hurlstone et al., 2003; Walsh and Stainier, 2001) (Fig. 1I-K, see Fig. S2A in the supplementary material). In *frv* mutants, none of these markers became properly restricted (Fig. 1L-N, see Fig. S2B in the supplementary material): *notch1b* expression was evident in the ventricular endocardium, *bmp4* expression was expanded into the ventricular myocardium, and *versican* and *tbx2b* expression expanded into both the ventricular and atrial myocardium. Additionally, *frv* mutants exhibited expanded localization of the adhesion molecule Dm-grasp. Dm-grasp is normally detectable in differentiated endocardial cells within the AVC, but not in the remainder of the endocardium (Beis et al., 2005) (Fig. 1O-Q). In *frv* mutants, Dm-grasp was found throughout the entire ventricular endocardium, as well as in the AVC endocardium (Fig. 1R-T). Thus, the presence of ectopic atrioventricular characteristics in the *frv* mutant ventricle indicates an important role for *frv* in the regional restriction of atrioventricular differentiation.

Positional cloning of *frv* reveals a novel transmembrane protein

To gain insight into the molecular mechanisms of *frv* function, we positionally cloned the gene encoded by the *frv* locus. Meiotic mapping of *frv* identified a 0.28 cM genetic interval, and the annotated zebrafish genome assembly indicated five candidate genes in this region (Fig. 2A). Examination of the coding sequence of one of these genes, *transmembrane protein 2* (*tmem2*), revealed a nonsense mutation in *frv* mutant genomic DNA that is predicted to truncate the Tmem2 protein (Fig. 2B). To test the hypothesis that loss of *tmem2* function is responsible for the *frv* mutant phenotype, we injected *tmem2* mRNA into *frv* mutant embryos and found that this can rescue the *frv* mutant defects in chamber morphology, ventricular contractility and Dm-grasp distribution (see Table S1 and Fig. S3G-I in the supplementary material). Injection of *tmem2* mRNA did not cause any detectable phenotype in wild-type embryos. Additionally, we found that injection of anti-*tmem2* morpholinos (MOs) into wild-type embryos could cause

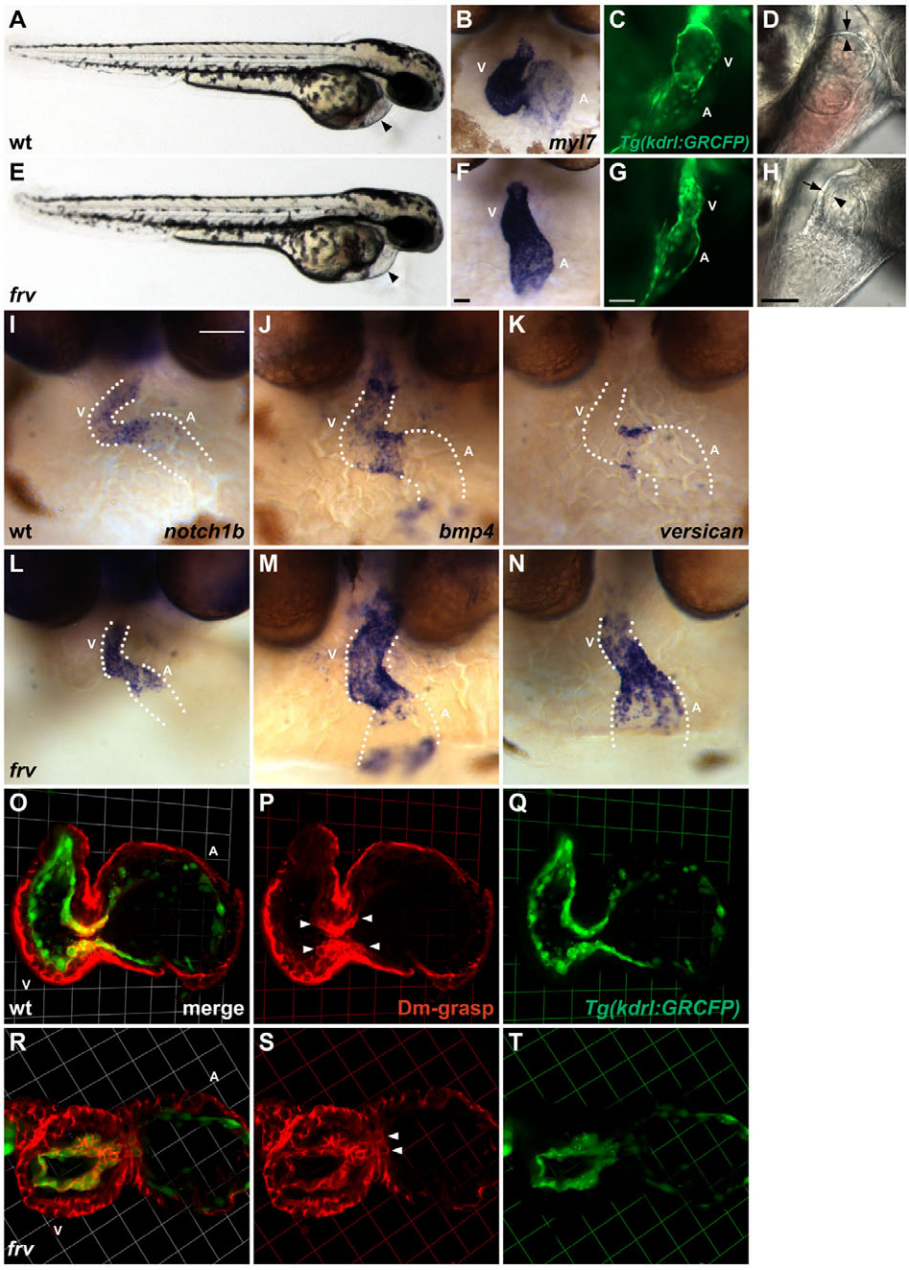

Fig. 1. The *frv* mutation disrupts myocardial and endocardial morphogenesis. (**A**,**E**) Lateral views of wild-type (wt) and *frv* mutant zebrafish embryos at 48 hpf reveal mild pericardial edema in *frv* mutants (arrowheads). Other than their cardiac defects, *frv* mutants appear morphologically normal. (**B**,**F**) Frontal views depict *myl7* expression in wild type (B) and in *frv* mutants (F) at 48 hpf. (**C**,**G**) Lateral views showing endocardial expression of *Tg(kdrl:GRCFP)* in wild type (C) and in *frv* mutants (G) at 52 hpf. (**D**,**H**) Lateral views at 52 hpf depict the close juxtaposition of the ventricular endocardium (arrowhead) and myocardium (arrow) in wild type (D) and their greater separation in *frv* mutants (H). (**I-N**) Frontal views depict expression of atrioventricular canal (AVC) markers in wild type (I-K) and in *frv* mutants (L-N) at 48 hpf. Dotted lines outline the chambers flanking the AVC. (**O-T**) Three-dimensional projections of selected confocal sections of wild-type (O-Q) and *frv* mutant (R-T) hearts expressing *Tg(kdrl:GRCFP)* (green) in the endocardium at 57 hpf. Immunofluorescence reveals Dm-grasp (red) throughout the myocardium and in the AVC endocardium (arrowheads). In *frv* mutants, Dm-grasp is also seen ectopically in the ventricular endocardium. Grids are 23 μm per segment. A, atrium; V, ventricle. Scale bars: 50 μm.

dysmorphic chambers, reduced ventricular contractility and ectopic Dm-grasp (see Fig. S3J-L in the supplementary material). Together, the linkage, nonsense mutation, rescue and MO phenocopy data indicate that disruption of the *tmem2* gene is the cause of the *frv* phenotype.

Tmem2 is predicted to be a type II transmembrane protein with a single transmembrane helix, a short cytoplasmic tail and a long extracellular portion (Fig. 2B). A BLAST local alignment search detected two identifiable domains – a G8 domain and a GG domain – within the extracellular sequence (Fig. 2B), consistent with previous bioinformatic analysis of the human TMEM2 homolog (see Fig. S4 in the supplementary material) (Guo et al., 2006; He et al., 2006). The structure of Tmem2 is highly conserved: Tmem2 homologs are detectable in a wide variety of vertebrate genomes, including *Homo sapiens*, *Mus musculus*, *Gallus gallus*, *Xenopus tropicalis* and *Takifugu rubripes*, all of which share at least 63% amino acid similarity with zebrafish Tmem2 (see Fig. S4 in the supplementary material). However, we were unable to identify Tmem2 homologs in *Caenorhabditis elegans* or *Drosophila melanogaster*. Despite its conservation among vertebrates, no prior studies have investigated Tmem2 function. Thus, our data provide novel evidence of an essential role for Tmem2.

Endocardial expression of *tmem2* represses inappropriate atrioventricular differentiation

The *frv* phenotype indicates that Tmem2 prevents atrioventricular differentiation in the ventricular endocardium, but it is not clear in which tissue Tmem2 acts to execute this role. Human and mouse Tmem2 homologs are expressed in a wide array of tissues (Scott et al., 2000). Consistent with this, we found broad expression of *tmem2* throughout the early zebrafish embryo, and we also detected a maternal supply of *tmem2* (see Fig. S5 in the supplementary material).

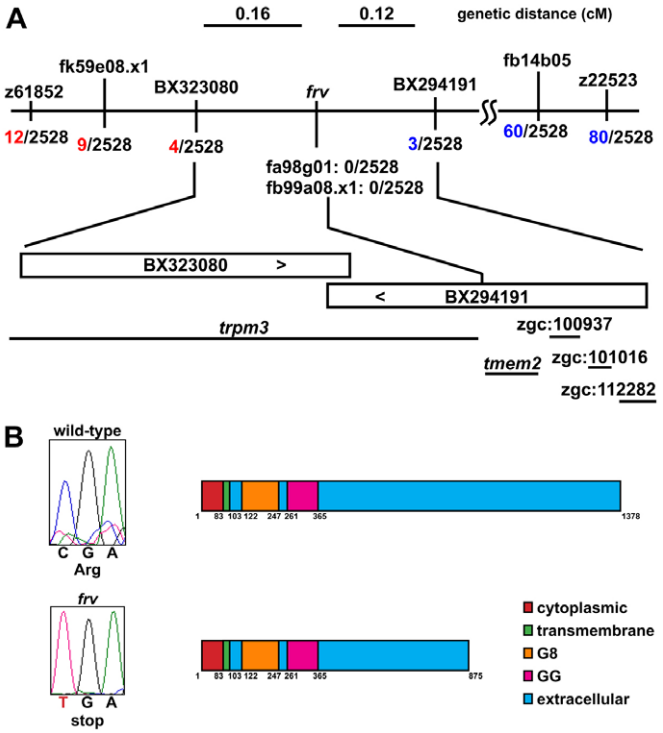

Fig. 2. The *frv* locus encodes the transmembrane protein Tmem2. (**A**) Meiotic and physical maps of the zebrafish genomic region containing *frv*. Meiotic mapping revealed a 0.28 cM interval for *frv* defined by SNPs on the ends of overlapping contigs (BX323080, BX294191). Fractions indicate the number of proximal (red) and distal (blue) recombination events out of 2528 meioses. Five candidate genes are shown as represented in Ensembl. (**B**) The predicted structures of Tmem2 protein in wild-type and *frv* mutant embryos. Amino acid positions defining the domains are indicated. Histograms demonstrate that *frv* mutants contain a C-to-T transition at position 2623 of the *tmem2* coding region. This mutation changes an Arg codon to a premature stop codon at amino acid position 875 and is predicted to result in a truncated Tmem2 protein.

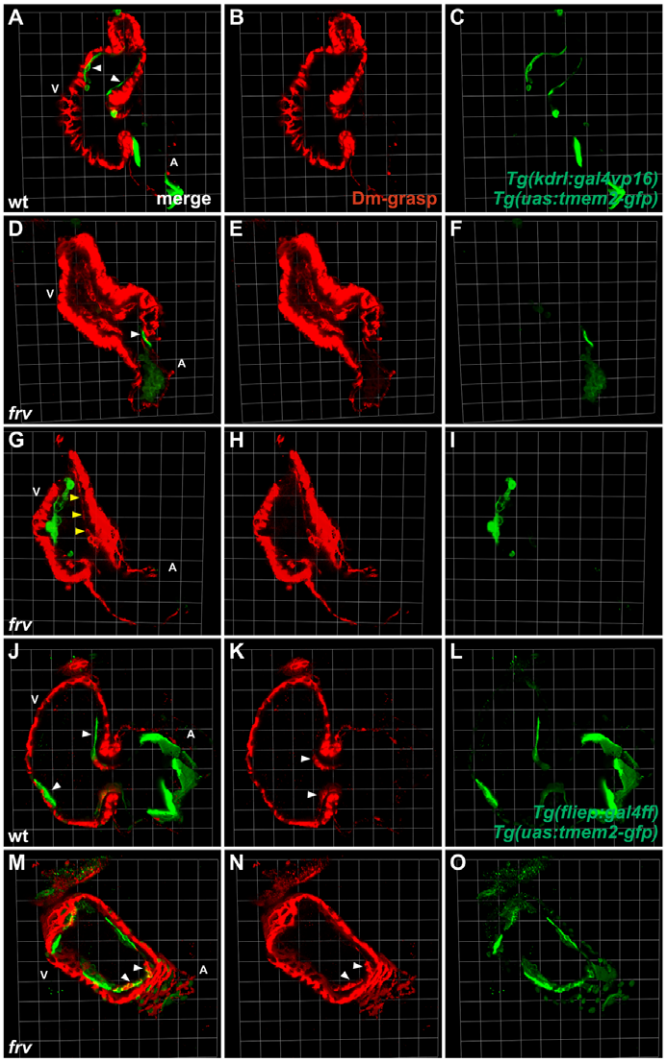

Fig. 3. Endocardial expression of *tmem2* rescues the *frv* mutant endocardium. Three-dimensional projections of selected confocal sections of wild-type (A-C,J-L) and *frv* mutant (D-I,M-O) zebrafish hearts expressing *tmem2-gfp* (green) in the endocardium at 57 hpf. Immunofluorescence indicates Dm-grasp localization (red). (A-I) Transient mosaic expression of *tmem2-gfp* is driven by injection of the transgenes *Tg(kdrl:gal4vp16)* and *Tg(uas:tmem2-gfp)*. (J-O) Mosaic expression of *tmem2-gfp* is driven by stably integrated *Tg(fliep:gal4ff)* and *Tg(uas:tmem2-gfp)* transgenes. (**A-C**,**J-L**) Expression of *tmem2-gfp* in ventricular endocardium (A,J, arrowheads) does not affect wild-type development. (**D-F**) Ectopic Dm-grasp remains in the *frv* mutant ventricle when *tmem2-gfp* is expressed only in atrial endocardium (D, arrowhead). (**G-I**) Mosaic expression of *tmem2-gfp* in the ventricular endocardium of *frv* mutants suppresses ectopic Dm-grasp localization. Ventricular endocardium that does not express *tmem2-gfp* retains ectopic Dm-grasp (G, arrowheads). (**M-O**) Broad *tmem2-gfp* expression in the ventricular endocardium rescues ectopic Dm-grasp expression in an *frv* mutant. AVC endocardium still expresses Dm-grasp as in wild type (compare M,N with K, arrowheads). Endocardial expression of *tmem2-gfp* does not improve ventricular contractility, but does reduce the abnormal gap between the myocardium and endocardium. Grids are 23 μm per segment.

Since the expression pattern of *tmem2* does not clarify its site of action, we designed tissue-specific transgenes to test whether expression of *tmem2* in the myocardium or endocardium could rescue the *frv* mutant phenotype. These transgenes drive expression of a fusion protein in which the C-terminus of Tmem2 is tagged with GFP. Tmem2-GFP appears functionally equivalent to Tmem2: injection of *tmem2-gfp* mRNA yielded results similar to injection of *tmem2* mRNA (see Table S1 in the supplementary material).

Expression of *tmem2* throughout the myocardium, driven by the stably integrated transgene *Tg(myl7:tmem2-gfp)* (see Fig. S6A-C in the supplementary material), was not sufficient to rescue the ectopic atrioventricular characteristics in *frv* mutants (see Fig. S7 in the supplementary material). Expression of *tmem2* in the endocardium was more challenging to attain. Since no endocardium-specific driver is available, we employed endothelial drivers (Jin et al., 2005; Villefranc et al., 2007). First, we used the transgenes *Tg(kdrl:gal4vp16)* and *Tg(uas:tmem2-gfp)* to generate transient mosaic expression within the endocardium (Fig. 3A-C). Expression of *tmem2* in atrial endocardium did not alter the *frv* mutant phenotype (Fig. 3D-F; n=4). By contrast, we observed loss of ectopic Dm-grasp in ventricular endocardial cells exhibiting mosaic *tmem2* expression (Fig. 3G-I; n=5). In an effort to generate a more thorough rescue of the *frv* endocardium, we next employed the stably integrated driver *Tg(fliep:gal4ff)* (Zygmunt et al., 2011). Unfortunately, stable integration of both *Tg(fliep:gal4ff)* and *Tg(uas:tmem2-gfp)* did not result in uniform expression of *tmem2* throughout the endocardium (Fig. 3J-L, see Fig. S6D in the

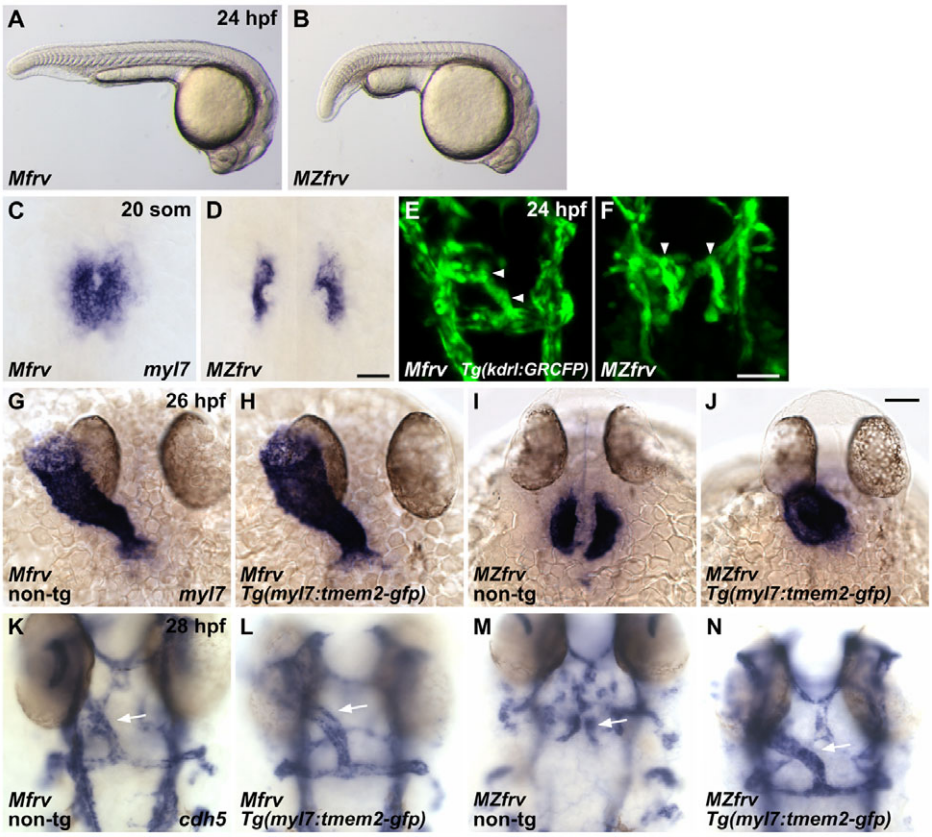

Fig. 4. Maternal-zygotic *frv* mutants exhibit myocardial and endocardial fusion defects that are rescued by myocardial *tmem2* expression. (**A**,**B**) Lateral views of zebrafish maternal (*Mfrv*) and maternal-zygotic (*MZfrv*) *frv* mutant siblings reveal body length and yolk extension defects in *MZfrv* embryos at 24 hpf. (**C**,**D**,**G-J**) Dorsal views depict *myl7* expression at 20 somites (som) and 26 hpf. (**E**,**F**) Dorsal views depict endocardial expression of *Tg(kdrl:GRCFP)* (arrowheads) at 24 hpf. (**K-N**) Dorsal views depict endocardial expression of *cdh5* (arrows) at 28 hpf In *Mfrv* embryos, expression of *Tg(myl7:tmem2-gfp)* has no effect on myocardial or endocardial morphogenesis (G,H,K,L), whereas in *MZfrv* embryos expression of *Tg(myl7:tmem2-gfp)* rescues both myocardial and endocardial fusion (I,J,M,N). Non-transgenic (non-tg) and transgenic siblings were distinguished by examination of fluorescence before fixation. Comparable results were obtained with two independent transgenic founders. Scale bars: 50 μm.

supplementary material), potentially owing to epigenetic silencing of *Tg(uas:tmem2-gfp)* (Goll et al., 2009). Accordingly, the effects of this transgene combination in *frv* mutants were comparable to the effects of mosaic expression of *Tg(kdrl:gal4vp16)* and *Tg(uas:tmem2-gfp)* (*n*=3); however, in one *frv* mutant, broad expression of *tmem2* in the ventricular endocardium eliminated the ectopic Dm-grasp (Fig. 3M-O). These data indicate that the activity of Tmem2 in the ventricular endocardium is sufficient to prevent the ectopic assumption of atrioventricular characteristics. Moreover, our data imply the existence of repressive mechanisms that restrain atrioventricular differentiation in the ventricle.

Tmem2 facilitates medial migration of both myocardium and endocardium

Given the contrast between the broad expression pattern of *tmem2* and the specific defects in *frv* mutants, we suspected that the maternal supply of *tmem2* partially compensates for the loss of zygotic *tmem2* function. To uncover additional roles of *tmem2*, we generated maternal-zygotic *frv* (*MZfrv*) mutant embryos via germline replacement (Ciruna et al., 2002). *MZfrv* mutants underwent gastrulation normally and began to display morphological defects during somitogenesis; by contrast, maternal *frv* (*Mfrv*) mutants appeared normal (Fig. 4A,B, see Fig. S8 in the supplementary material). Cardiac defects emerged in *MZfrv* mutants at an earlier stage than in zygotic *frv* mutants. Whereas cardiac fusion proceeded normally in *Mfrv* mutants, the medial migration of *MZfrv* cardiomyocytes was significantly hindered (Fig. 4C,D). However, the bilateral populations of cardiomyocytes were not permanently separated, and they eventually formed two linked sets of dysmorphic chambers (see Fig. S9 in the supplementary material). Additionally, *MZfrv* mutants displayed abnormal endocardial migration. Instead of meeting at the midline to form an endocardial tube, *MZfrv* endocardial cells were substantially delayed in their medial migration and remained bilaterally separate (Fig. 4E,F). Therefore, Tmem2 is crucial for facilitating cell movement during cardiac fusion.

Myocardial expression of *tmem2* promotes both myocardial and endocardial fusion

The failure of both myocardial and endocardial fusion in *MZfrv* mutants suggested the possibility that both phenotypes result from a primary defect in endoderm formation. However, endodermal specification and morphogenesis appeared normal in *MZfrv* mutants (data not shown). We therefore hypothesized that Tmem2 functions in migrating cardiac cells. Using the stably integrated transgene *Tg(myl7:tmem2-gfp)*, we found that myocardial expression of *tmem2* could rescue myocardial migration in *MZfrv* mutants; although morphogenesis was still slightly delayed in rescued embryos, cardiac fusion was complete and heart tube extension was under way by 26 hpf (Fig. 4G-J, see Fig. S10A-D in the supplementary material; *n*=15). Remarkably, the positive effects of *Tg(myl7:tmem2-gfp)* expression extended to the endocardium. Myocardial expression of *tmem2* rescued endocardial migration in *MZfrv* mutants, such that the endocardial cells reached the midline and extended into a tube (Fig. 4K-N, see Fig. S10E-H in the supplementary material; *n*=12). These data demonstrate that Tmem2 activity in the myocardium is sufficient to facilitate both myocardial and endocardial fusion. Moreover, our data provide the first evidence for a myocardial factor that influences the migration of endocardial cells.

Tmem2 is essential for the coordination of myocardial and endocardial morphogenesis

Our studies provide the first demonstration that the previously unappreciated transmembrane protein Tmem2 has multiple important functions during development. Notably, Tmem2 is

essential for two crucial aspects of cardiac morphogenesis: the spatial restriction of atrioventricular differentiation during AVC formation and the medial migration of cardiac cells during cardiac fusion. In each context, we have identified one location where Tmem2 can function – in the endocardium during AVC formation and in the myocardium during cardiac fusion – although our results do not rule out additional sites for Tmem2 activity during these processes. Our data suggest intriguing mechanisms for the coordination of myocardial and endocardial morphogenesis by Tmem2, and it is attractive to speculate that Tmem2 might play similar roles during AVC differentiation and cardiac fusion.

The transmembrane localization of Tmem2 evokes the hypothesis that it could facilitate myocardium-endocardium signaling. Perhaps certain signals repress atrioventricular differentiation in the ventricle, and Tmem2 plays a permissive role in facilitating signal reception by the endocardium. Similarly, Tmem2 could act to limit the activity of inductive signals that specify AVC endocardium; for example, the similarities between *frv* mutants and *apc* mutants suggest a possible role of Tmem2 in restricting Wnt signaling (Hurlstone et al., 2003; Verhoeven et al., 2011). During cardiac fusion, Tmem2 might facilitate the transduction of an unknown myocardial-to-endocardial motility cue; however, this scenario seems unlikely because the endocardium can move to the midline in *hand2* mutants, which possess very few cardiomyocytes (Garavito-Aguilar et al., 2010). Alternatively, rather than influencing specific signaling pathways, Tmem2 might impact myocardial and endocardial morphogenesis by modulating the extracellular environment. Perhaps Tmem2 influences ECM organization between the endocardium and myocardium in a manner that normally insulates the ventricular endocardium from myocardial signals that induce atrioventricular differentiation. Likewise, since specific parameters of ECM composition are known to be fundamental for cardiac fusion (Arrington and Yost, 2009; Garavito-Aguilar et al., 2010; Trinh and Stainier, 2004), Tmem2 could play a permissive role in ensuring the appropriate ECM organization to facilitate both myocardial and endocardial movement. Whatever the molecular role of Tmem2, its activity, as described here, broadens our comprehension of the mechanisms that underlie the coordination of myocardial and endocardial development. Elucidating the biochemical basis for Tmem2 function will further advance our understanding of the roles of this novel developmental regulator.

Note added in proof

An accompanying paper (Smith et al., 2011) characterizes the phenotype caused by zebrafish mutations referred to as *wickham* (*wkm*) and reports that the *wkm* locus encodes *tmem2*. Complementation tests performed by breeding *frv* heterozygotes to *wkm* heterozygotes have demonstrated that the two mutant alleles fail to complement each other: summarizing the results of five independent clutches, 27.7% (49/177) of the progeny display a phenotype indistinguishable from that of zygotic *frv* mutants. These data further reinforce the conclusion that the *frv* and *wkm* mutations disrupt the same gene: *tmem2*.

Acknowledgements

We thank L. Pandolfo, K. McCrone, E. Reynolds and C. McDaniel for expert zebrafish care, and T. J. Cardozo, T. Evans, D. Fitch, A. Joyner, H. Knaut and members of the Yelon laboratory for constructive discussions.

Funding

Work in the Yelon laboratory is supported by grants from the National Institutes of Health, American Heart Association and March of Dimes. Deposited in PMC for release after 12 months.

Competing interests statement

The authors declare no competing financial interests.

Supplementary material

Supplementary material for this article is available at http://dev.biologists.org/lookup/suppl/doi:10.1242/dev.064261/-/DC1

References

Alexander, J., Stainier, D. Y. and Yelon, D. (1998). Screening mosaic F1 females for mutations affecting zebrafish heart induction and patterning. *Dev. Genet.* **22**, 288-299.

Armstrong, E. J. and Bischoff, J. (2004). Heart valve development: endothelial cell signaling and differentiation. *Circ. Res.* **95**, 459-470.

Arrington, C. B. and Yost, H. J. (2009). Extra-embryonic syndecan 2 regulates organ primordia migration and fibrillogenesis throughout the zebrafish embryo. *Development* **136**, 3143-3152.

Beis, D., Bartman, T., Jin, S. W., Scott, I. C., D'Amico, L. A., Ober, E. A., Verkade, H., Frantsve, J., Field, H. A., Wehman, A. et al. (2005). Genetic and cellular analyses of zebrafish atrioventricular cushion and valve development. *Development* **132**, 4193-4204.

Bussmann, J., Bakkers, J. and Schulte-Merker, S. (2007). Early endocardial morphogenesis requires Scl/Tal1. *PLoS Genet.* **3**, e140.

Chi, N. C., Shaw, R. M., De Val, S., Kang, G., Jan, L. Y., Black, B. L. and Stainier, D. Y. (2008). Foxn4 directly regulates tbx2b expression and atrioventricular canal formation. *Genes Dev.* **22**, 734-739.

Ciruna, B., Weidinger, G., Knaut, H., Thisse, B., Thisse, C., Raz, E. and Schier, A. (2002). Production of maternal-zygotic mutant zebrafish by germ-line replacement. *Proc. Natl. Acad. Sci. USA* **99**, 14919-14924.

Cross, L. M., Cook, M. A., Lin, S., Chen, J. N. and Rubinstein, A. L. (2003). Rapid analysis of angiogenesis drugs in a live fluorescent zebrafish assay. *Arterioscler. Thromb. Vasc. Biol.* **23**, 911-912.

Fisher, S., Grice, E. A., Vinton, R. M., Bessling, S. L., Urasaki, A., Kawakami, K. and McCallion, A. S. (2006). Evaluating the biological relevance of putative enhancers using Tol2 transposon-mediated transgenesis in zebrafish. *Nat. Protoc.* **1**, 1297-1305.

Garavito-Aguilar, Z. V., Riley, H. E. and Yelon, D. (2010). Hand2 ensures an appropriate environment for cardiac fusion by limiting fibronectin function. *Development* **137**, 3215-3220.

Goll, M. G., Anderson, R., Stainier, D. Y., Spradling, A. C. and Halpern, M. E. (2009). Transcriptional silencing and reactivation in transgenic zebrafish. *Genetics* **182**, 747-755.

Guo, J., Cheng, H., Zhao, S. and Yu, L. (2006). GG: a domain involved in phage LTF apparatus and implicated in human MEB and non-syndromic hearing loss diseases. *FEBS Lett.* **580**, 581-584.

He, Q. Y., Liu, X. H., Li, Q., Studholme, D. J., Li, X. W. and Liang, S. P. (2006). G8: a novel domain associated with polycystic kidney disease and non-syndromic hearing loss. *Bioinformatics* **22**, 2189-2191.

Hinton, R. B. and Yutzey, K. E. (2010). Heart valve structure and function in development and disease. *Annu. Rev. Physiol.* **73**, 29-46.

Holtzman, N. G., Schoenebeck, J. J., Tsai, H. J. and Yelon, D. (2007). Endocardium is necessary for cardiomyocyte movement during heart tube assembly. *Development* **134**, 2379-2386.

Hurlstone, A. F., Haramis, A. P., Wienholds, E., Begthel, H., Korving, J., Van Eeden, F., Cuppen, E., Zivkovic, D., Plasterk, R. H. and Clevers, H. (2003). The Wnt/beta-catenin pathway regulates cardiac valve formation. *Nature* **425**, 633-637.

Jin, S. W., Beis, D., Mitchell, T., Chen, J. N. and Stainier, D. Y. (2005). Cellular and molecular analyses of vascular tube and lumen formation in zebrafish. *Development* **132**, 5199-5209.

Kikuchi, Y., Agathon, A., Alexander, J., Thisse, C., Waldron, S., Yelon, D., Thisse, B. and Stainier, D. Y. (2001). casanova encodes a novel Sox-related protein necessary and sufficient for early endoderm formation in zebrafish. *Genes Dev.* **15**, 1493-1505.

Kupperman, E., An, S., Osborne, N., Waldron, S. and Stainier, D. Y. (2000). A sphingosine-1-phosphate receptor regulates cell migration during vertebrate heart development. *Nature* **406**, 192-195.

Kwan, K., Fujimoto, E., Grabher, C., Mangum, B., Hardy, M., Campbell, D., Parant, J., Yost, H., Kanki, J. and Chien, C. (2007). The Tol2kit: a multisite gateway-based construction kit for Tol2 transposon transgenesis constructs. *Dev. Dyn.* **236**, 3088-3099.

Mjaatvedt, C. H., Lepera, R. C. and Markwald, R. R. (1987). Myocardial specificity for initiating endothelial-mesenchymal cell transition in embryonic chick heart correlates with a particulate distribution of fibronectin. *Dev. Biol.* **119**, 59-67.

Moreno-Rodriguez, R. A., Krug, E. L., Reyes, L., Villavicencio, L., Mjaatvedt, C. H. and Markwald, R. R. (2006). Bidirectional fusion of the heart-forming fields in the developing chick embryo. *Dev. Dyn.* **235**, 191-202.

Schoenebeck, J. J., Keegan, B. R. and Yelon, D. (2007). Vessel and blood specification override cardiac potential in anterior mesoderm. *Dev. Cell* **13**, 254-267.

Scott, D. A., Drury, S., Sundstrom, R. A., Bishop, J., Swiderski, R. E., Carmi, R., Ramesh, A., Elbedour, K., Srikumari Srisailapathy, C. R., Keats, B. J. et al. (2000). Refining the DFNB7-DFNB11 deafness locus using intragenic polymorphisms in a novel gene, TMEM2. *Gene* **246**, 265-274.

Sedmera, D., Pexieder, T., Vuillemin, M., Thompson, R. P. and Anderson, R. H. (2000). Developmental patterning of the myocardium. *Anat. Rec.* **258**, 319-337.

Smith, K. A., Lagendijk, A. K., Courtney, A. D., Chen, H., Paterson, S., Hogan, B. M., Wicking, C. and Bakkers, J. (2011). Transmembrane protein 2 (Tmem2) is required to regionally restrict atrioventricular canal boundary and endocardial cushion development. *Development* **138**, 4193-4198.

Trinh, L. A. and Stainier, D. Y. (2004). Fibronectin regulates epithelial organization during myocardial migration in zebrafish. *Dev. Cell* **6**, 371-382.

Verhoeven, M. C., Haase, C., Christoffels, V. M., Weidinger, G. and Bakkers, J. (2011). Wnt signaling regulates atrioventricular canal formation upstream of BMP and Tbx2. *Birth Defects Res. A Clin. Mol. Teratol.* **91**, 435-440.

Villefranc, J. A., Amigo, J. and Lawson, N. D. (2007). Gateway compatible vectors for analysis of gene function in the zebrafish. *Dev. Dyn.* **236**, 3077-3087.

Walsh, E. C. and Stainier, D. Y. (2001). UDP-glucose dehydrogenase required for cardiac valve formation in zebrafish. *Science* **293**, 1670-1673.

Zygmunt, T., Gay, C. M., Blondelle, J., Singh, M. K., Flaherty, K. M., Means, P. C., Herwig, L., Krudewig, A., Belting, H.-G., Affolter, M. et al. (2011). Semaphorin-PlexinD1 signaling limits angiogenic potential via the VEGF decoy receptor sFlt1. *Dev. Cell* (in press).

Table S1. Injection of *tmem2* mRNA can rescue *frv* mutant embryos

Degree of rescue	Chamber morphology	Ventricular contractility	Dm-grasp restriction
Complete rescue	18/26 (69%)	24/26 (92%)	9/13 (69%)
Partial rescue	6/26 (23%)	0/26 (0%)	2/13 (15%)
No rescue	2/26 (8%)	2/26 (8%)	2/13 (15%)

Embryos were injected with *tmem2* mRNA at the one-cell stage; *frv* mutant embryos were identified by PCR genotyping. Of the 26 mutant embryos identified, 92% exhibited normal ventricular contractility, 69% exhibited normal chamber morphology, and 23% exhibited partial rescue of chamber morphology. We examined Dm-grasp immunofluorescence in a subset of the injected embryos. Of the 13 mutant embryos examined, 85% exhibited complete or partial elimination of Dm-grasp from the ventricular endocardium (see Fig. S3G-I in the supplementary material). We presume that the variability in phenotypic rescue reflects inconsistency in the stability of the injected mRNA.